

# Inelastic light scattering near the Mott metal-insulator transition

**Jim Freericks** (Georgetown University)

*Funding:* **National Science Foundation**

**Civilian Research and Development Foundation**

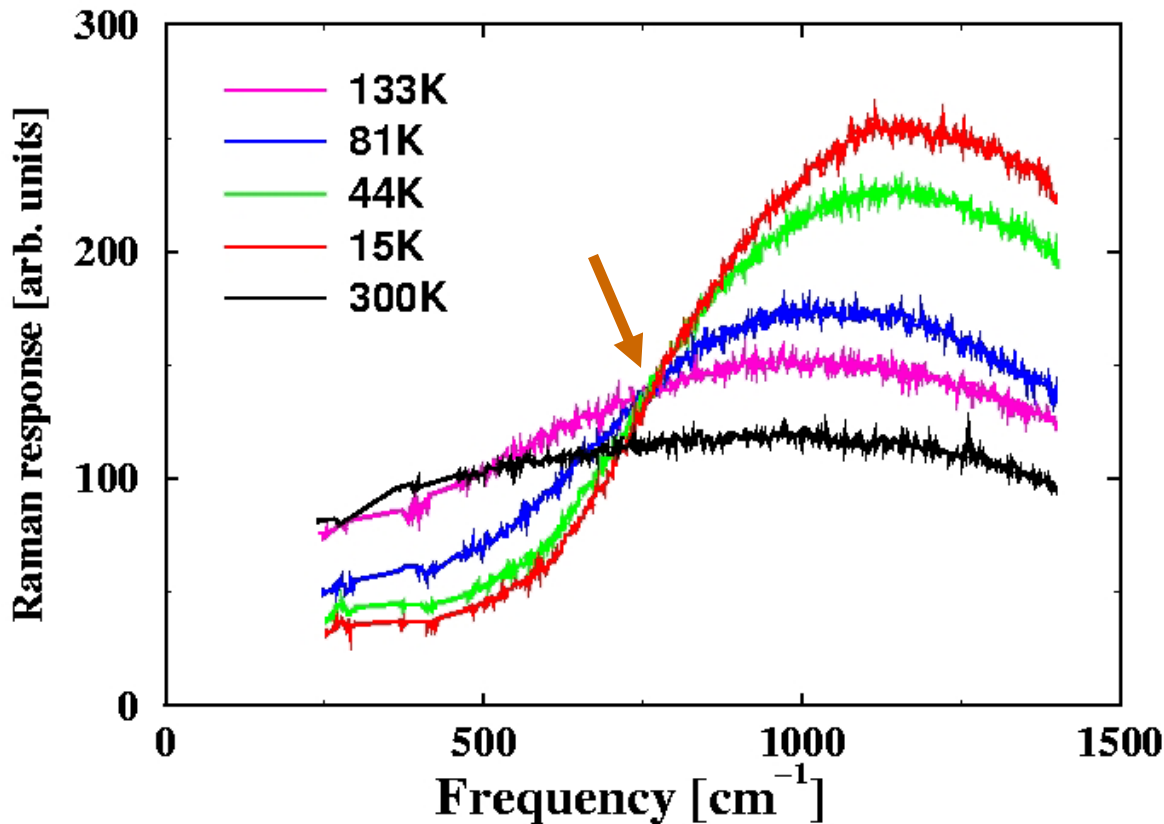
*In collaboration with:* Tom Devereaux, Andrij Shvaika, Oleg Vorobyov, Lance Cooper, and Ralf Bulla

*Thanks to:* Rudi Hackl, Zahid Hasan, Paul Miller, Z.-X. Shen, and Michel van Veenendal

# Raman scattering probes electronic excitations

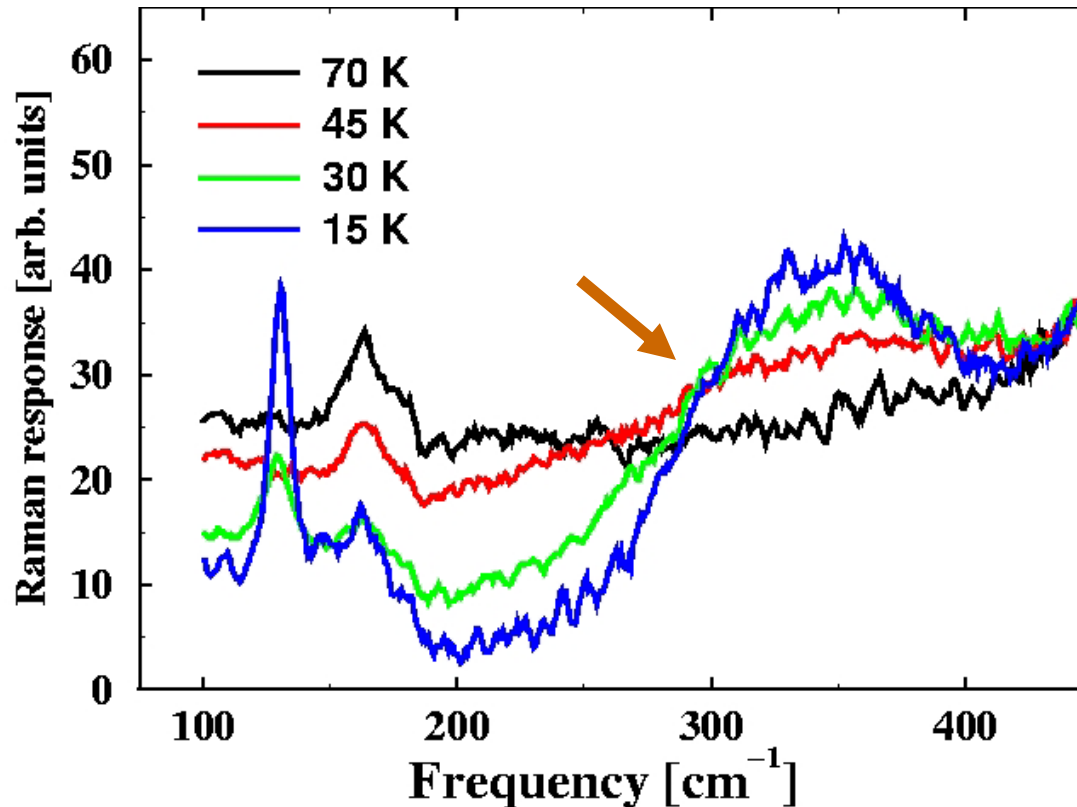
- **Inelastic scattering of light** with electron-hole excitations of the correlated many-body system.
- Use of polarizers for the incident and reflected light allows one to **select different symmetries** of the electron-hole excitations.
- Signal depends on the **Raman scattering amplitude  $\gamma(\mathbf{k})$** . We consider three different symmetries here:
- $A_{1g}$ :  $\gamma(\mathbf{k}) \sim \cos(k_x a) + \cos(k_y a)$
- $B_{1g}$ :  $\gamma(\mathbf{k}) \sim \cos(k_x a) - \cos(k_y a)$
- $B_{2g}$ :  $\gamma(\mathbf{k}) \sim \sin(k_x a) \sin(k_y a)$  [vanishes for nn hopping]

# Experimental data for Kondo insulators



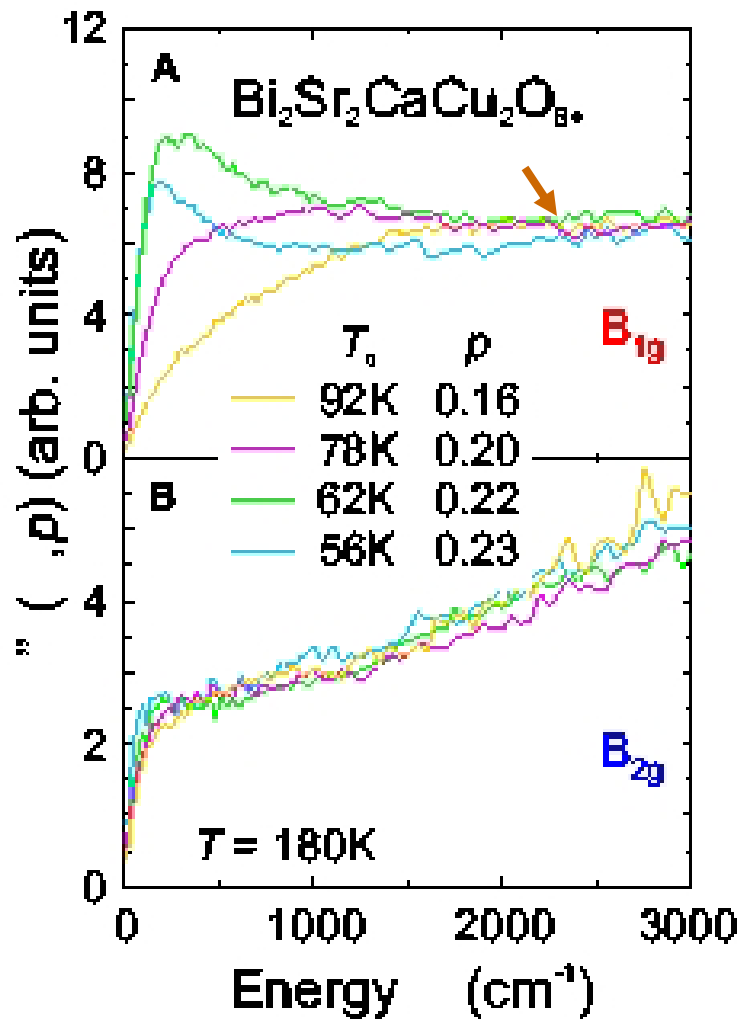
- *Nyhus et al, PRB 95* Raman scattering on **FeSi**. Note the appearance of the **isosbestic point** below about 150K.
- The low frequency spectral weight is **reduced** and the higher frequency weight is **enhanced** as the temperature is lowered.

# Experimental data for intermediate-valence materials



- *Nyhus et al, 1995 and 1997* Raman scattering on  $\text{SmB}_6$ . Note the appearance of the **isosbestic point** near  $300 \text{ cm}^{-1}$ .
- Below 30K, there is an **increase** in low frequency spectral weight in a narrow peak at about  $130 \text{ cm}^{-1}$ .

# Experimental data for high T<sub>c</sub> superconductors



- *Venturini et al.* PRL 2002, Raman scattering on BSCCO as a function of doping at constant temperature (180 K).
- Note how the B<sub>1g</sub> and B<sub>2g</sub> results **agree** in the overdoped regime, but they **differ** as the system becomes more underdoped (and hence more correlated).

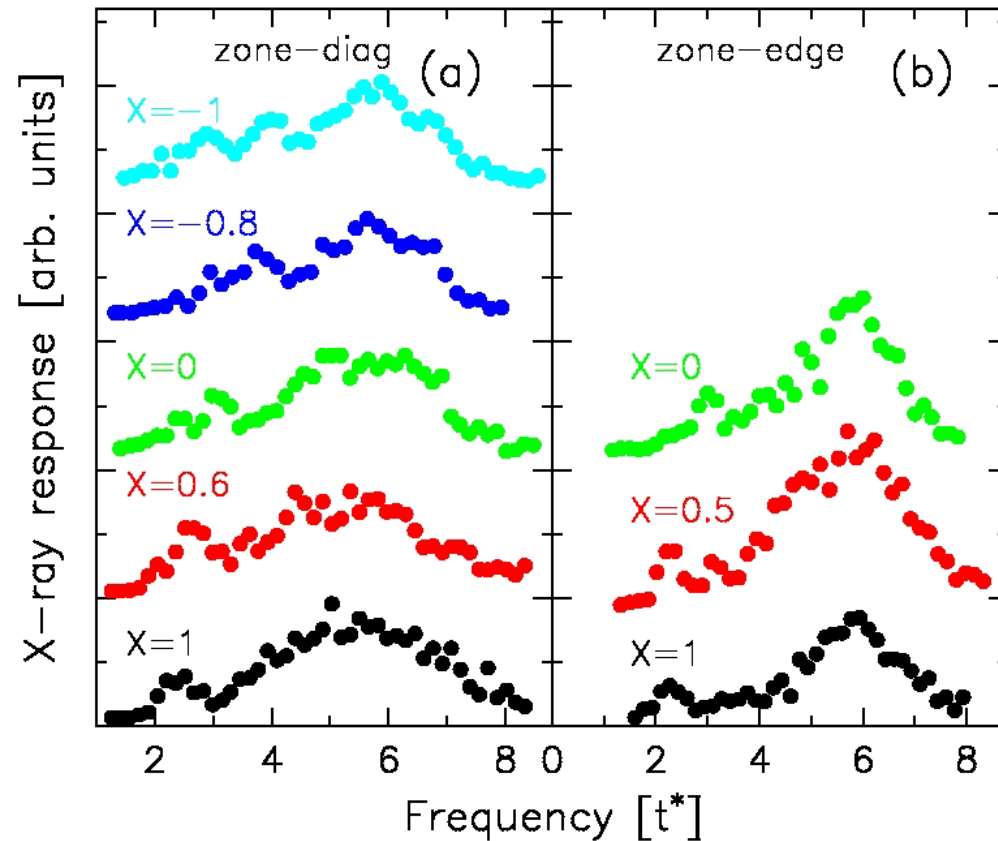
# Summary of Experimental Data (Raman)

- Three characteristic behaviors are seen: (i) as  $T$  is lowered, there is a **redistribution of spectral weight** from low-frequency to high frequency; (ii) these regions are separated by an isosbestic point, where **the Raman response is independent** of  $T$ ; (iii) the ratio of the twice spectral range where spectral weight is depleted to the onset temperature, where it first is reduced, is **much larger than 3.5** (typically 10-30).
- For correlated insulators this behavior is “**universal**” in the sense that it **does not depend** on the microscopic properties of the insulating phase, be it a Kondo insulator or an intermediate-valence material or a high  $T_c$  superconductor.

# Resonant Inelastic X-ray Scattering probes momentum and energy dependent charge excitations

- By **tuning** the photon energy to the K or L<sub>3</sub> edge of a core state, one finds large enhancements to the inelastic scattering.
- Advanced light sources have linearly polarized light, but experiments to date have not used (crossed) polarizers on the detectors. Hence **different symmetry channels are mixed together** in the experimental results.
- The scattered signal depends on the **Raman scattering amplitude  $\gamma(\mathbf{k}+\mathbf{q}/2)$**  for transferred momentum  $\mathbf{q}$ .
- The energy resolution in current experiments is poor (**about 0.1 eV**) but is expected to improve dramatically with second-generation experiments (**less than 20 meV**).

# RIXS on $\text{CaCu}_2\text{O}_2\text{Cl}_2$



RIXS data from Shen's group,  
Hasan et al., *Science* 2000.

Experimental data on a Mott insulator shows a **broad charge-transfer peak** and a **dispersive low-energy peak**.

We label the transferred momentum by the parameter  $X(\mathbf{q}) = [\cos q_x + \cos q_y]/2$ . When plotted in this fashion, the dispersion along the zone diagonal and zone center is **similar**.

The difference for  $X=1$  along the different zone axes occurs due to the relation between the polarization vector and  $\mathbf{q}$ , which **differs** for the different directions.



# Summary of Experimental Data (RIXS)

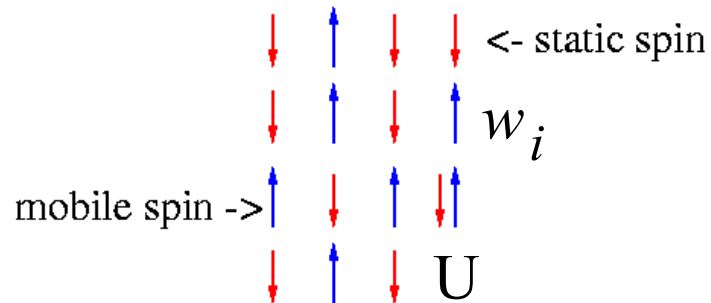
- RIXS experiments on correlated insulators typically show two features---(i) a **large-weight charge-transfer peak** and (ii) a **lower-energy peak**. The charge transfer peak shows **little dispersion** through the Brillouin zone, while the lower-energy peak **does disperse**. The dispersion from the zone center to zone corner is usually about **twice** the dispersion from the zone center to the zone edge boundary.
- Experimental results project onto different weights of the different symmetry channels due to a **locking of the photon momentum direction to the polarization of the electric field**.
- Systematic changes in temperature **have not been carried out yet**.

# Theories of inelastic light scattering

- The **insulating limit** has been analyzed by Chubukov and Frenkel (PRL, 1995).
- The **antiferromagnetically correlated metal** has been described by Devereaux and Kampf (PRB, 1999).
- Here we develop a theory that connects these two regimes and carries one through the **quantum critical point** of a metal-insulator transition.
- Experimental results exist for a variety of materials that pass through a **metal-insulator transition** as a function of doping.
- *Here we show how one can solve for Raman and inelastic X-ray scattering through a metal-insulator transition in both the Falicov-Kimball model and the Hubbard model.*

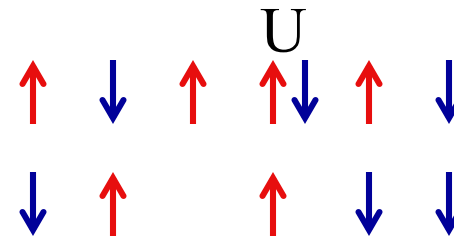
## Spinless Falicov-Kimball Model

$$H = -\frac{t}{2\sqrt{d}} \sum_{\langle i,j \rangle} c_i^\dagger c_j + E \sum_i w_i + U \sum_i c_i^\dagger c_i w_i$$



## Hubbard Model

$$H = -\frac{t}{2\sqrt{d}} \sum c_{i\sigma}^* c_{j\sigma} + U \sum n_{i\uparrow} n_{i\downarrow}$$



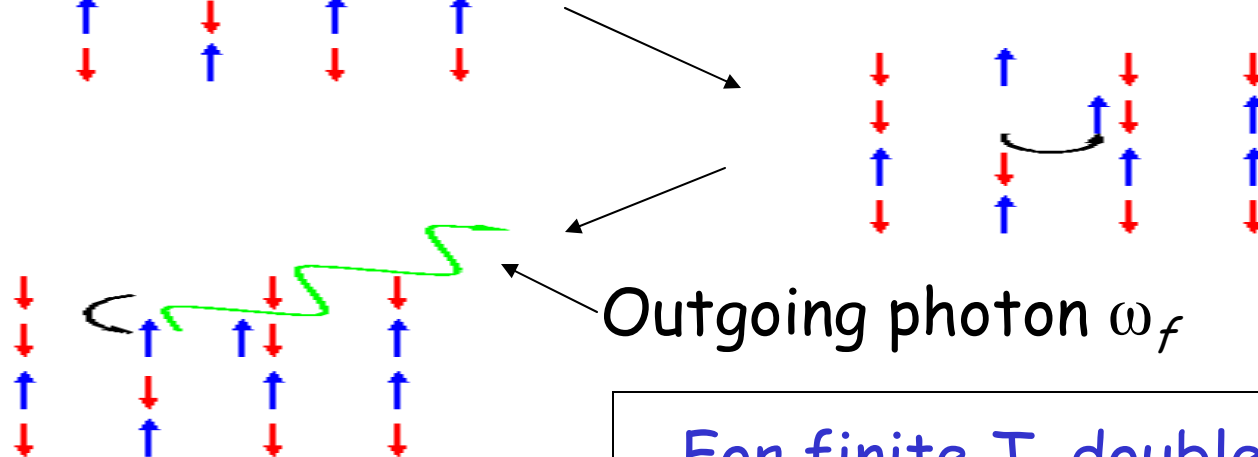
Both electrons are now mobile

- **exactly solvable model** on a hypercubic lattice in infinite dimensions using dynamical mean field theory.
- possesses homogeneous, commensurate/incommensurate CDW and SDW phases, phase segregation, and **metal-insulator transitions**.
- *Inelastic light scattering can be constructed formally exactly.*

# Light scattering processes

Incoming photon  $\omega_i$

Costs energy  $U$   
(charge transfer energy).

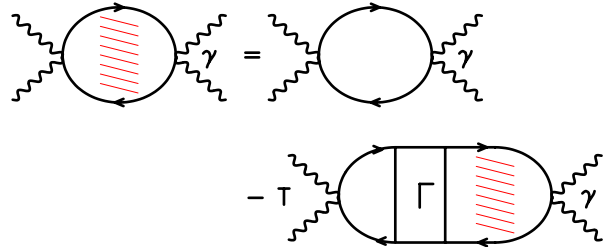
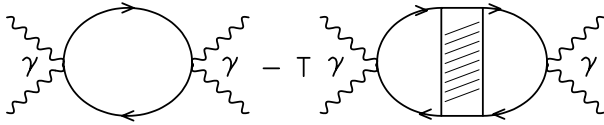


Electron hops,  
gains  $t$ .

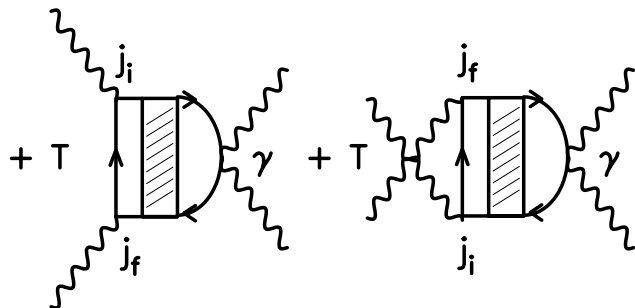
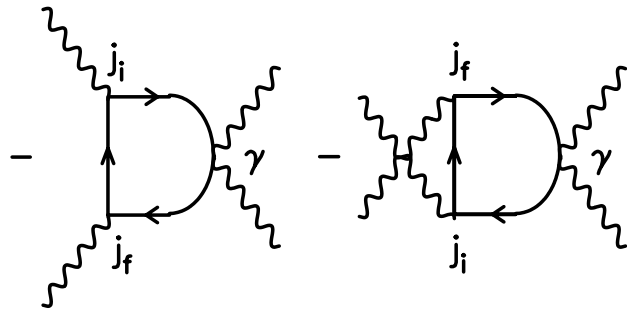
Outgoing photon  $\omega_f$

For finite  $T$ , double  
occupancies lead to  
small band of low  
energy electrons.

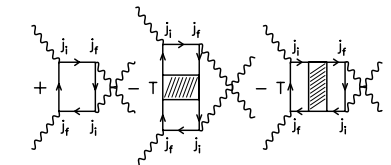
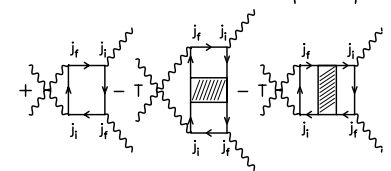
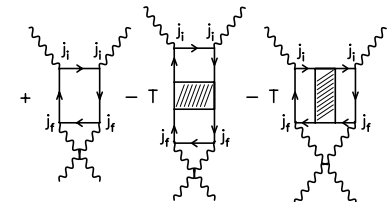
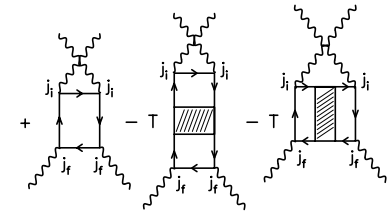
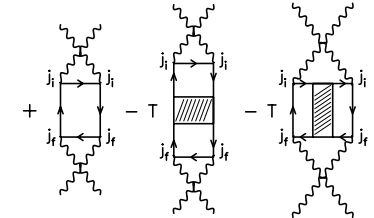
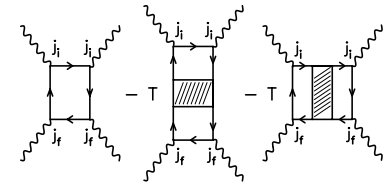
# Diagrammatics



Nonresonant



Mixed



Resonant

# Formal Solution for the Light Scattering Response

## $A_{1g}$ channel

- This channel has the **full symmetry** of the lattice
- The scattering response function contains **resonant, mixed and nonresonant** terms.
- The irreducible charge vertex for the Falicov-Kimball model is a **simple function** of the electronic self energy and Green's function (Shvaika, Physica C, 2000; Freericks and Miller, PRB, 2000). *This is **not** true for the Hubbard model.*
- The **nonresonant, mixed, and resonant** responses can be determined **exactly** by properly solving the relevant Dyson equations.
- We schematically show how to solve this problem using schematic **Feynman diagrams**.

# Diagrams for the nonresonant $A_{1g}$ response

$$\text{Diagram 1} = \text{Diagram 2} - T \text{Diagram 3}$$

Diagram 1: An oval with a vertical hatched bar on the left. The left half is labeled  $\gamma(k)$  and the right half is labeled  $\gamma(k')$ .

Diagram 2: An empty oval. The left half is labeled  $\gamma(k)$  and the right half is labeled  $\gamma(k)$ .

Diagram 3: An oval with a vertical grey bar in the center labeled  $\Gamma$ . The left half is labeled  $\gamma(k)$  and the right half is labeled  $\gamma(k')$ .

$$\text{Diagram 4} = \text{Diagram 5} - T \text{Diagram 6}$$

Diagram 4: An oval with a vertical hatched bar on the left. The right half is labeled  $\gamma(k)$ .

Diagram 5: An empty oval. The right half is labeled  $\gamma(k)$ .

Diagram 6: An oval with a vertical blue bar in the center labeled  $\Gamma$ . The right half is labeled  $\gamma(k)$ .

$\gamma(k) = -\epsilon(k)$ ,  $\Gamma$  is **local** and has no  $k$ -dependence

*Solving these coupled equations allows for the full nonresonant response to be determined.*

# Formal Solution for the Light Scattering Response

## $B_{1g}$ channel

- This channel is **orthogonal** to the lattice.
- There are **no vertex corrections** (Khurana, PRL, 1990), so the response is represented by the **bare bubble** (Raman response and X-ray response along the zone diagonal only).
- This Raman ( $\mathbf{q}=\mathbf{0}$ ) response is **identical** to that of the optical conductivity multiplied by one factor of frequency (Shastry and Shraiman, PRL, 1990).
- **Resonant** but not **mixed** scattering is possible in this channel.

*The nonresonant  $B_{1g}$  Raman response is closely related to the optical conductivity.*



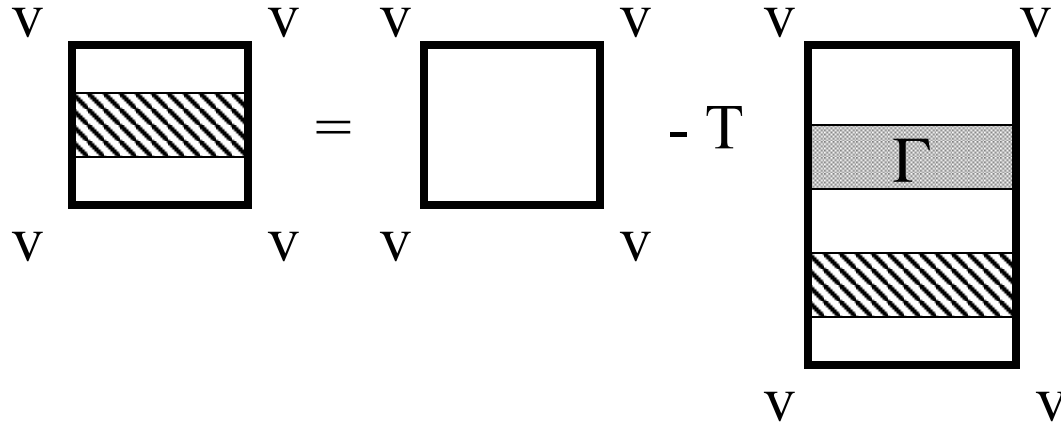
# Formal Solution for the Light Scattering Response

## $B_{2g}$ channel

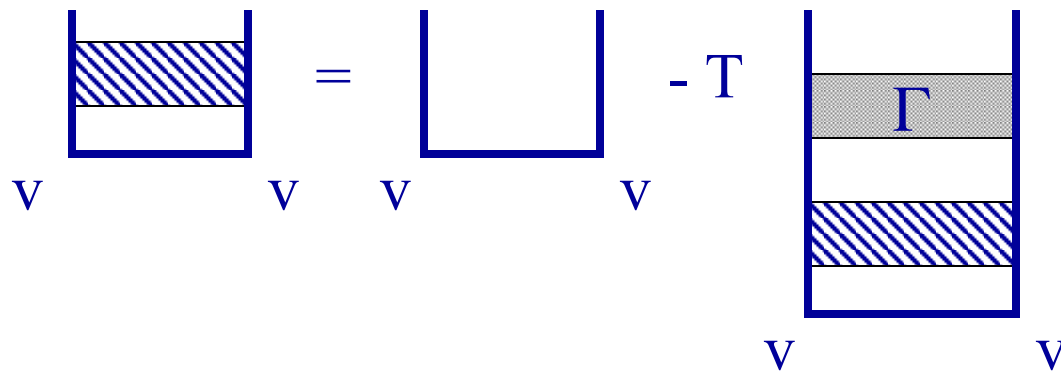
- The scattering amplitude vanishes for nearest neighbor hopping on a hypercubic lattice, so there are **no nonresonant or mixed responses**.
- The square of the current operator does contain  $B_{2g}$  symmetry, so **pure resonant processes are possible**.
- **Vertex corrections** are needed, but are relatively simple to handle.
- We describe how the resonant calculations can be performed in this channel.

*$B_{2g}$  Raman scattering is purely resonant.*

# Diagrams for the $B_{2g}$ resonant Raman response

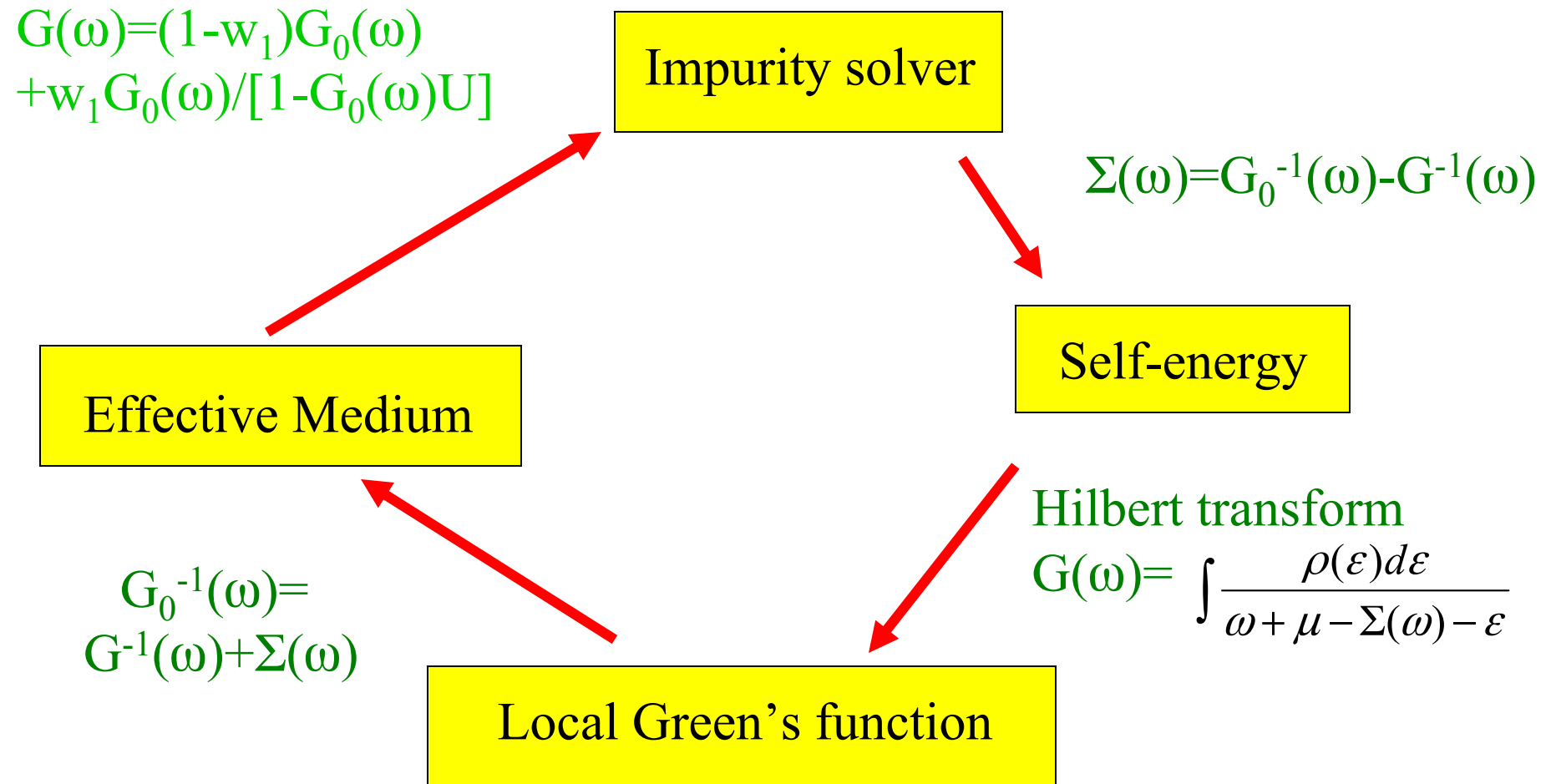


- In these diagrams, the vertex  $v$  is the **velocity operator**  $v(k)=d\varepsilon(k)/dk$  dotted into the photon polarization.



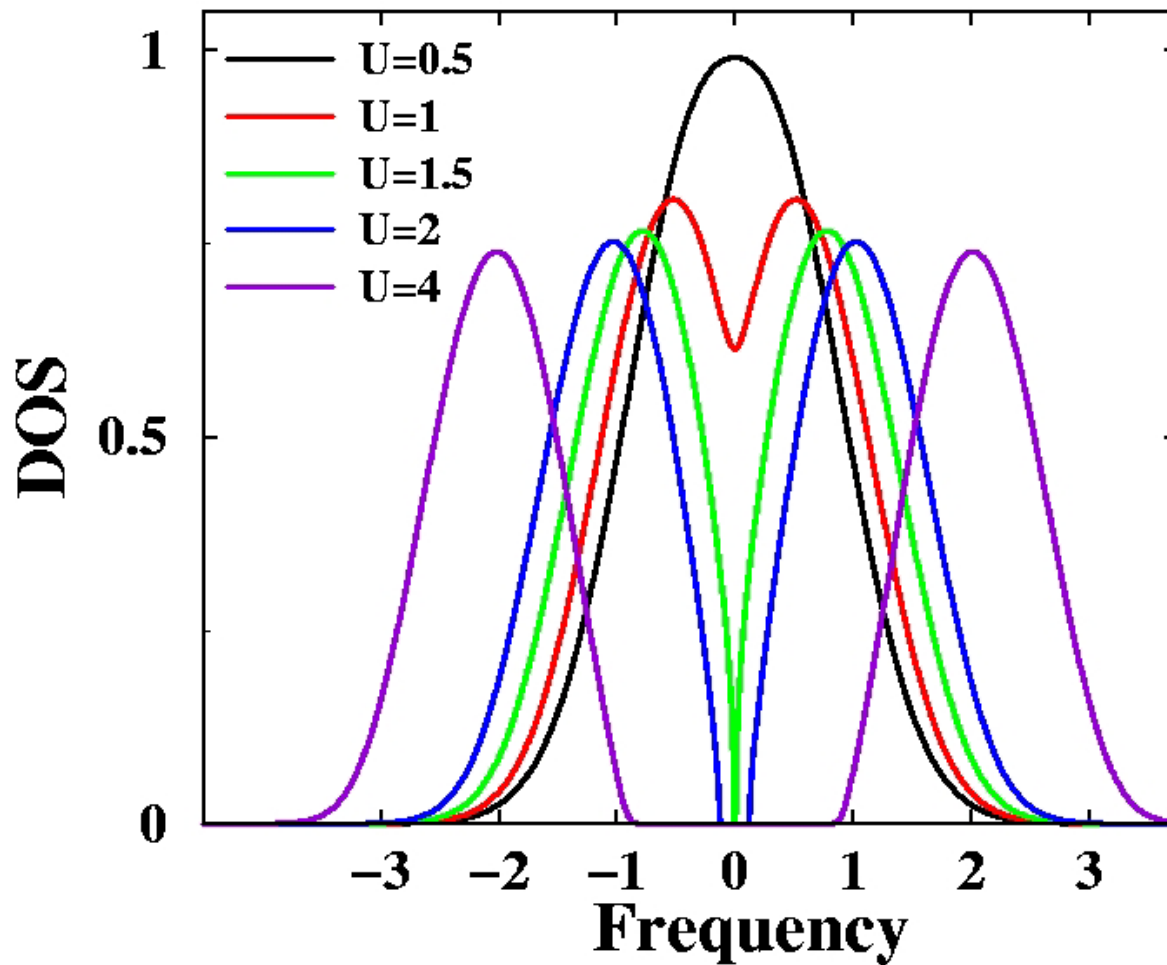
- These **coupled** Dyson equations must be solved together in order to get the resonant Raman response.

# Solving the many-body problem (FK model)



DMFT algorithm is iterated until a self-consistent solution is achieved

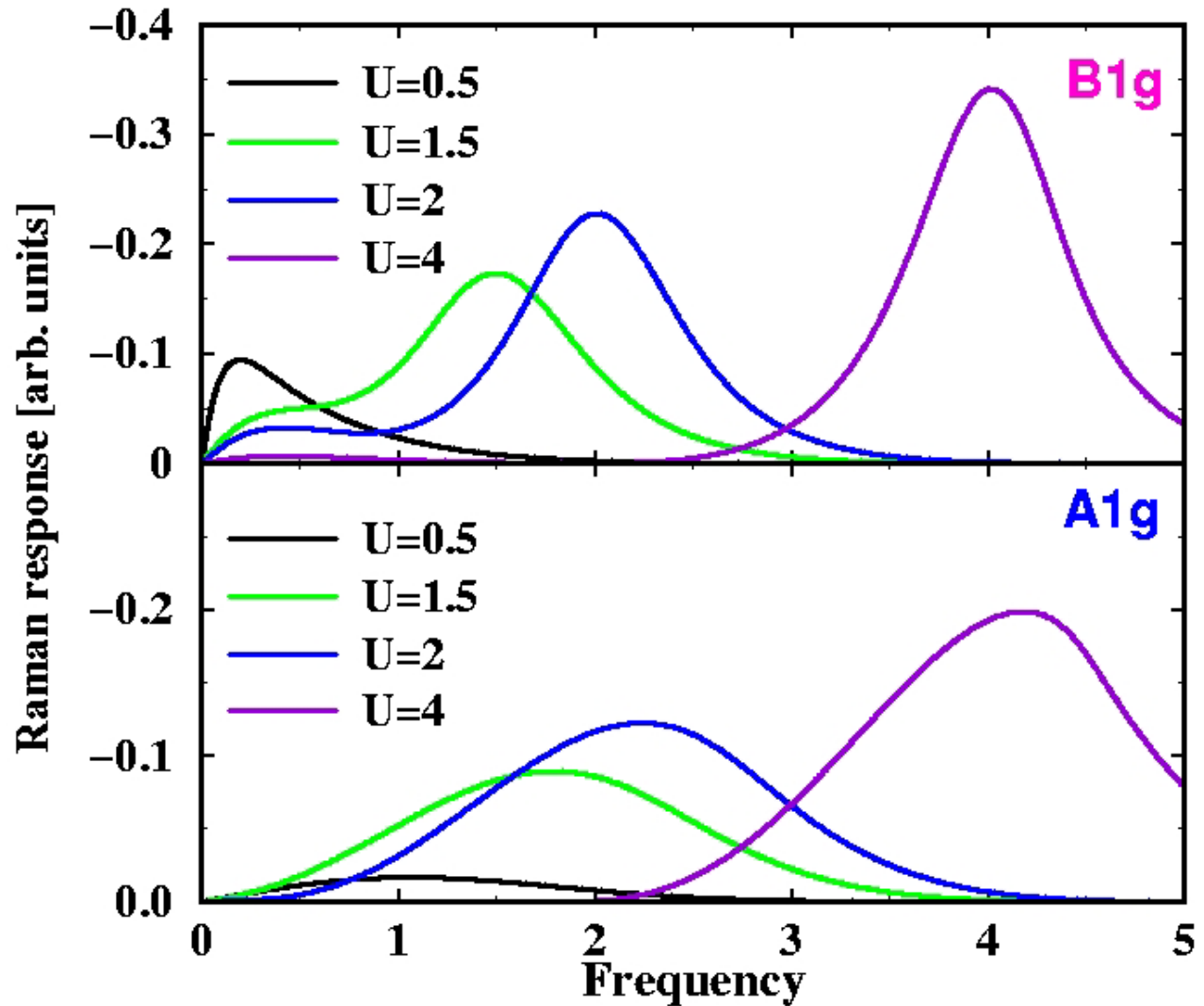
# FK model Metal-Insulator transition (NFL)



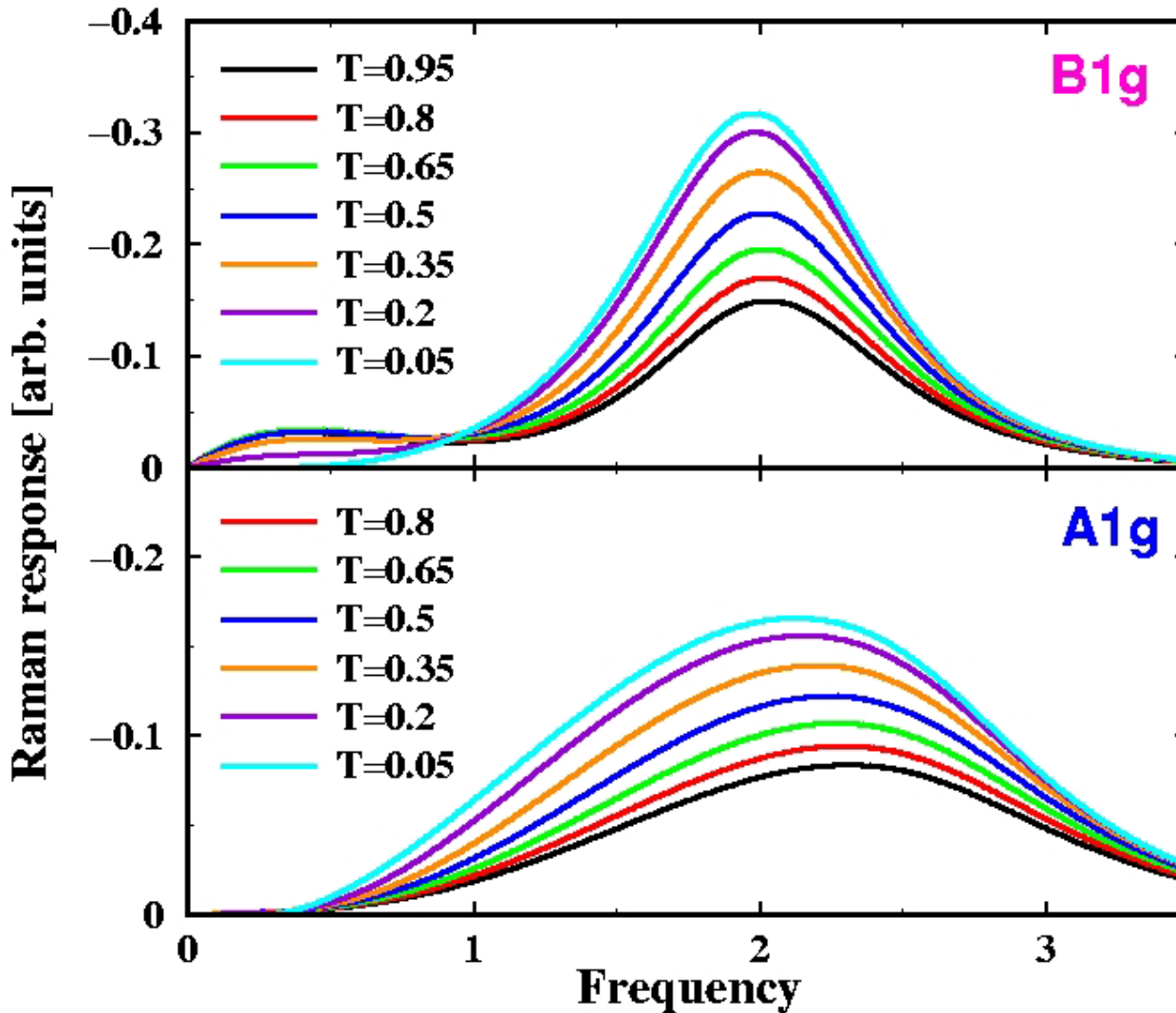
- **Correlation-induced** gap drives the single-particle DOS to zero at  $\omega=0$  for  $U>\sqrt{2}$
- Interacting DOS is **independent of  $T$**  in DMFT (Van Dongen, PRB, 1992)
- *Examine Raman response through the ( $T=0$ ) quantum phase transition.*

# Nonresonant Raman Response (Constant T)

- The  $A_{1g}$  response is suppressed at low frequencies, but the  $B_{1g}$  response displays low-frequency spectral weight as one passes through the **metal-insulator transition**.
- Note the **charge transfer peaks** for large  $U$ .



# Nonresonant Raman Response ( $U=2$ )

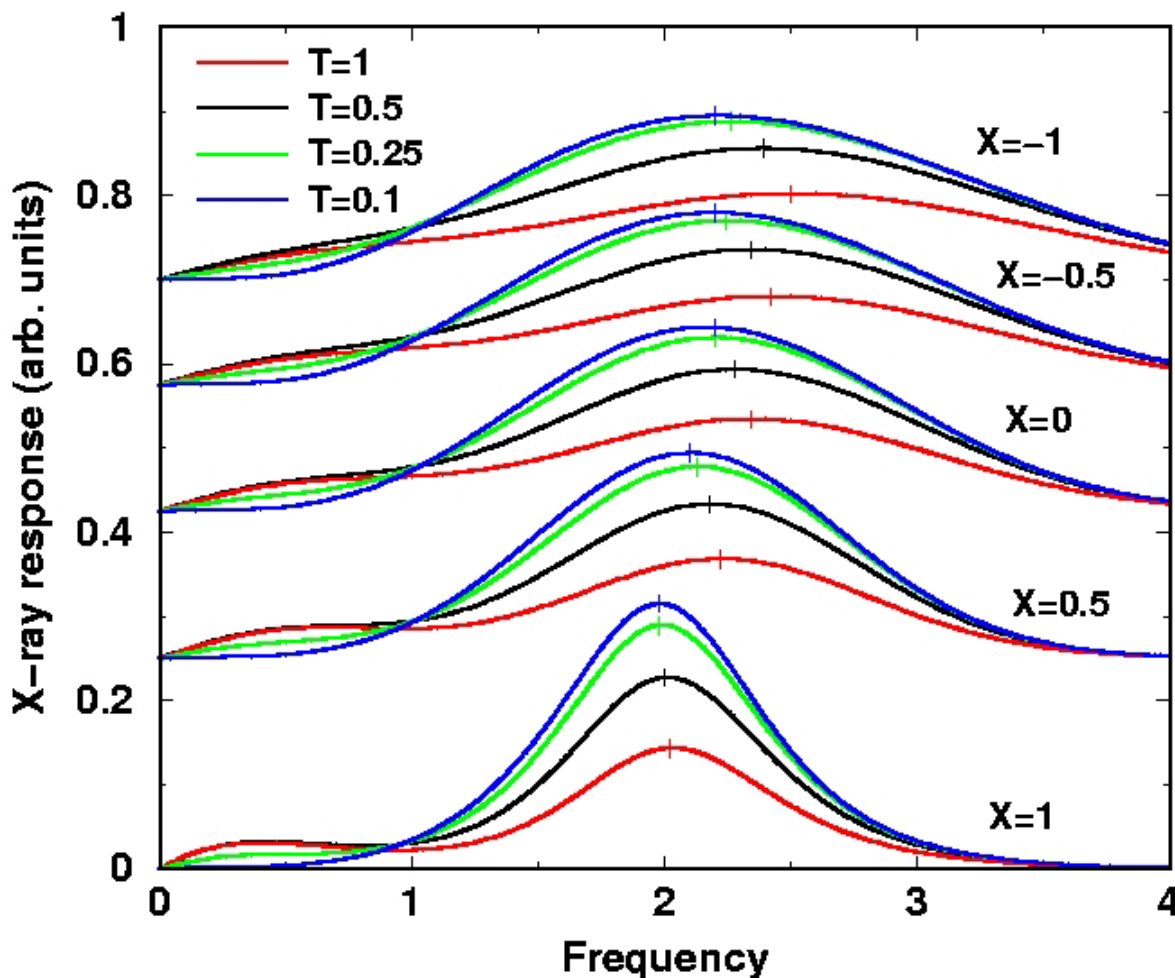


- The low-frequency  $B_{1g}$  response develops at a low temperature over a wide frequency range of  $O(1)$ .

- An **isosbestic point** divides where spectral weight increases or decreases as  $T$  is lowered ( $B_{1g}$ ).

# Inelastic X-ray scattering ( $B_{1g}$ )

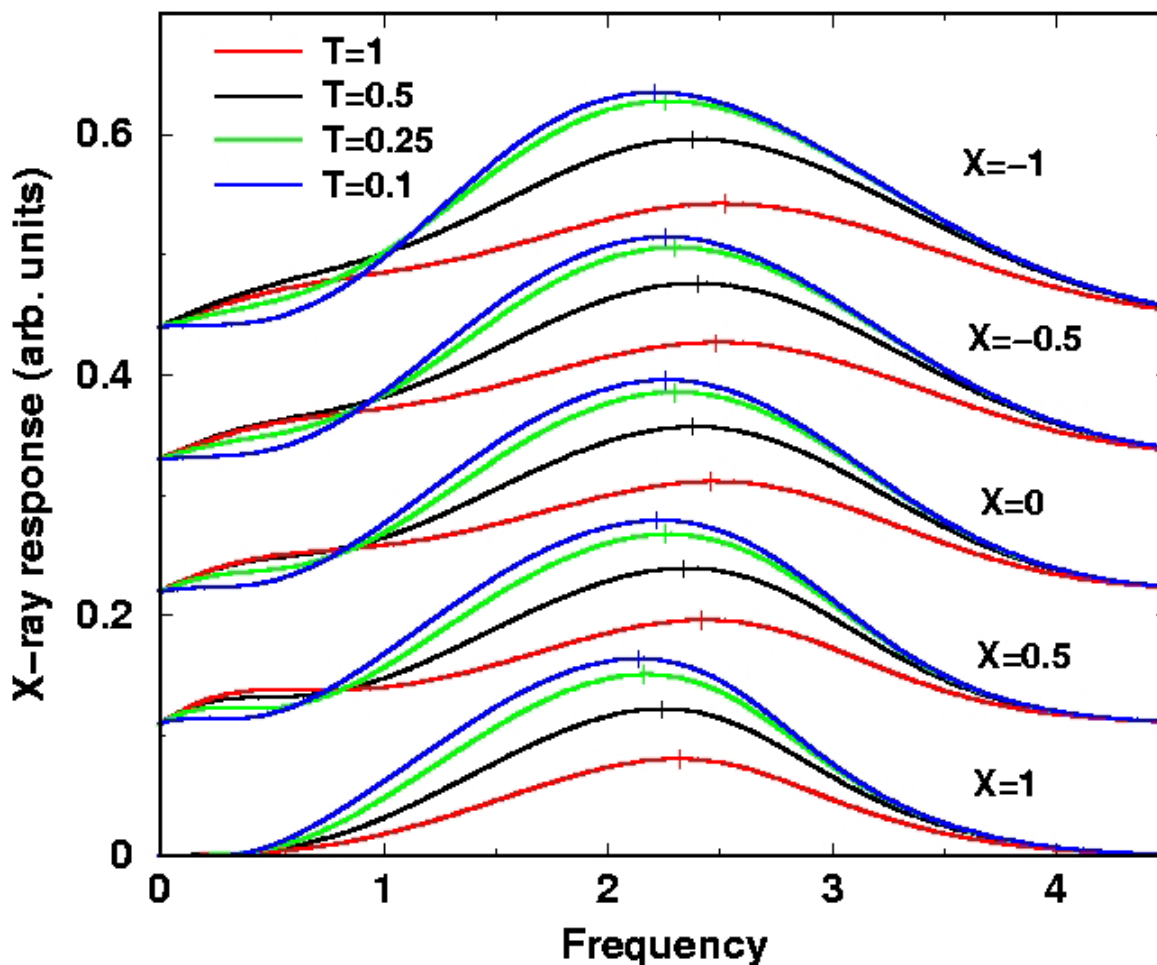
zone diagonal



- Scattering of x-rays allows the photon to exchange **both momentum and energy** with the electron-hole excitations.
- We see a **broadening and dispersion** of the peaks, but the **same** anomalous low-energy behavior and the isosbestic point.

# Inelastic X-ray scattering ( $A_{1g}$ )

zone diagonal

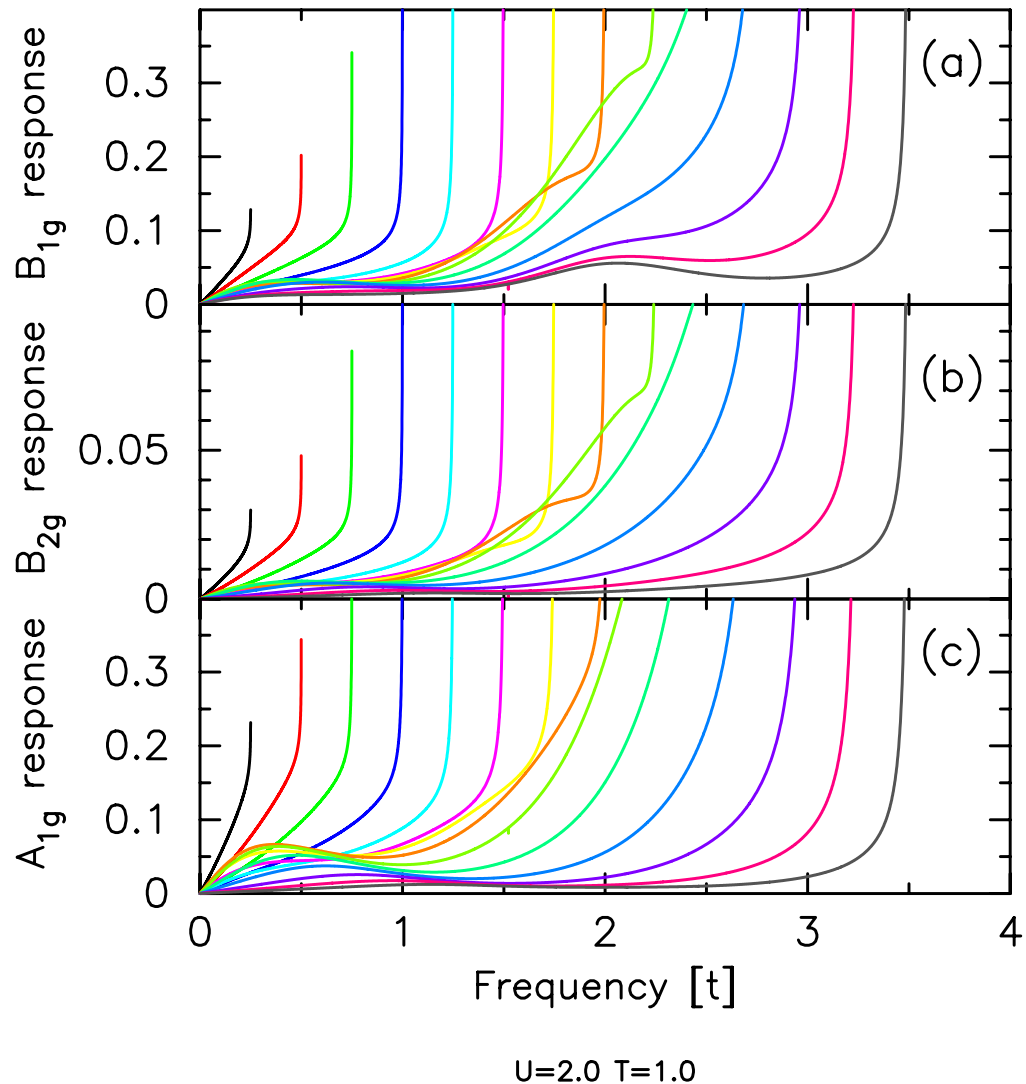


- Here the results at finite- $\mathbf{q}$  differ greatly from  $\mathbf{q}=\mathbf{0}$ : all of the anomalies appear away from  $\mathbf{q}=\mathbf{0}$ !
- A reduced **broadening** and **dispersion** of the peaks is seen; but the **same** anomalous low-energy behavior and the isosbestic points recur for nonzero  $\mathbf{q}$ .

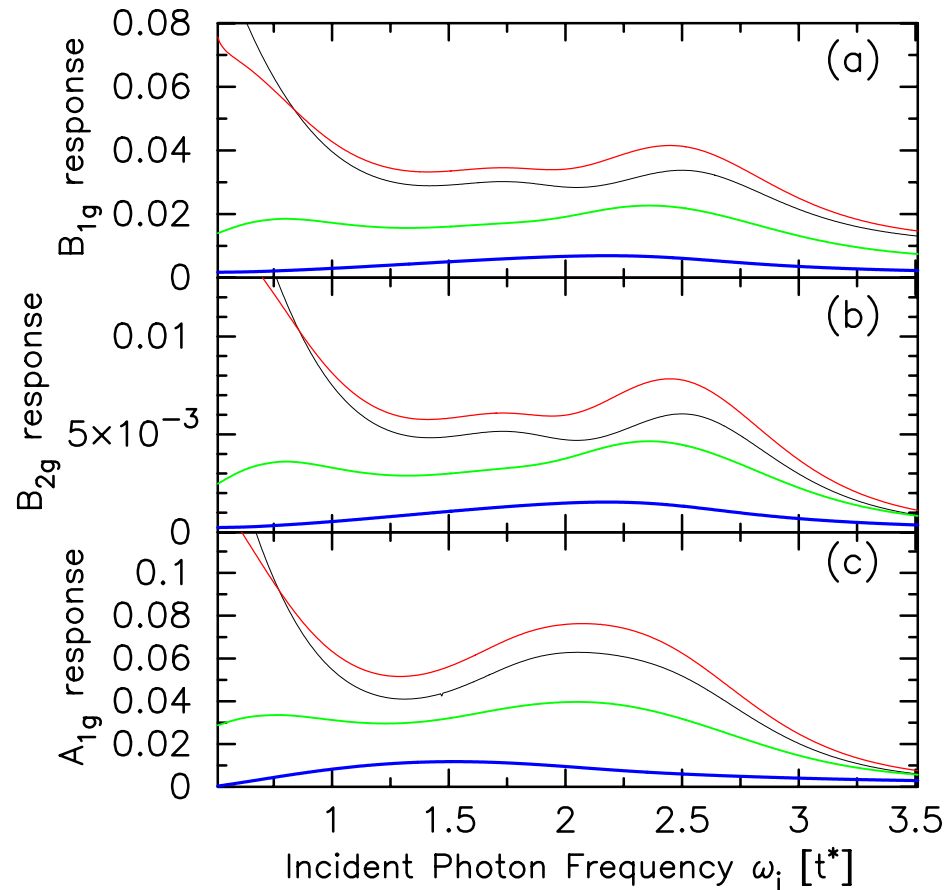


# Resonant effects

- There is a large **double resonance** when the transferred frequency approaches the incident photon frequency.
- The resonant effects can be large, and can **change the shape** of the nonresonant results when the photon frequency is close to either  $\Omega$  or  $U$ .



# Joint resonance effect



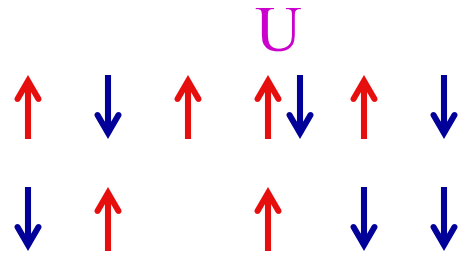
- When we examine the Raman signal at the low-energy peak, we find that it resonates when the photon frequency is close to it, and when it is close to  $U$ . The different colors are different temperatures.

# Summary (FK model)

- The theoretical results are **qualitatively similar** to experimental results measured in correlated systems.
- The nonresonant  $B_{1g}$  channel displays (i) an **isosbestic point** that divides the regions where the Raman response increase or decrease as  $T$  is lowered; (ii) a **sharp depletion of spectral weight** in the low-frequency region as  $T$  is reduced; and (iii) the temperature where low-frequency spectral features appear is **much lower than the range** in frequency over which those features appear.
- Results for inelastic light scattering are **model independent** on the insulating side of the MIT.
- Vertex corrections **suppress all nontrivial behavior** for the  $A_{1g}$  channel at  $\mathbf{q}=0$ .
- There is an interesting **joint resonance** of the high and low energy peaks when the initial photon frequency is close to  $U$ .

# Hubbard Model

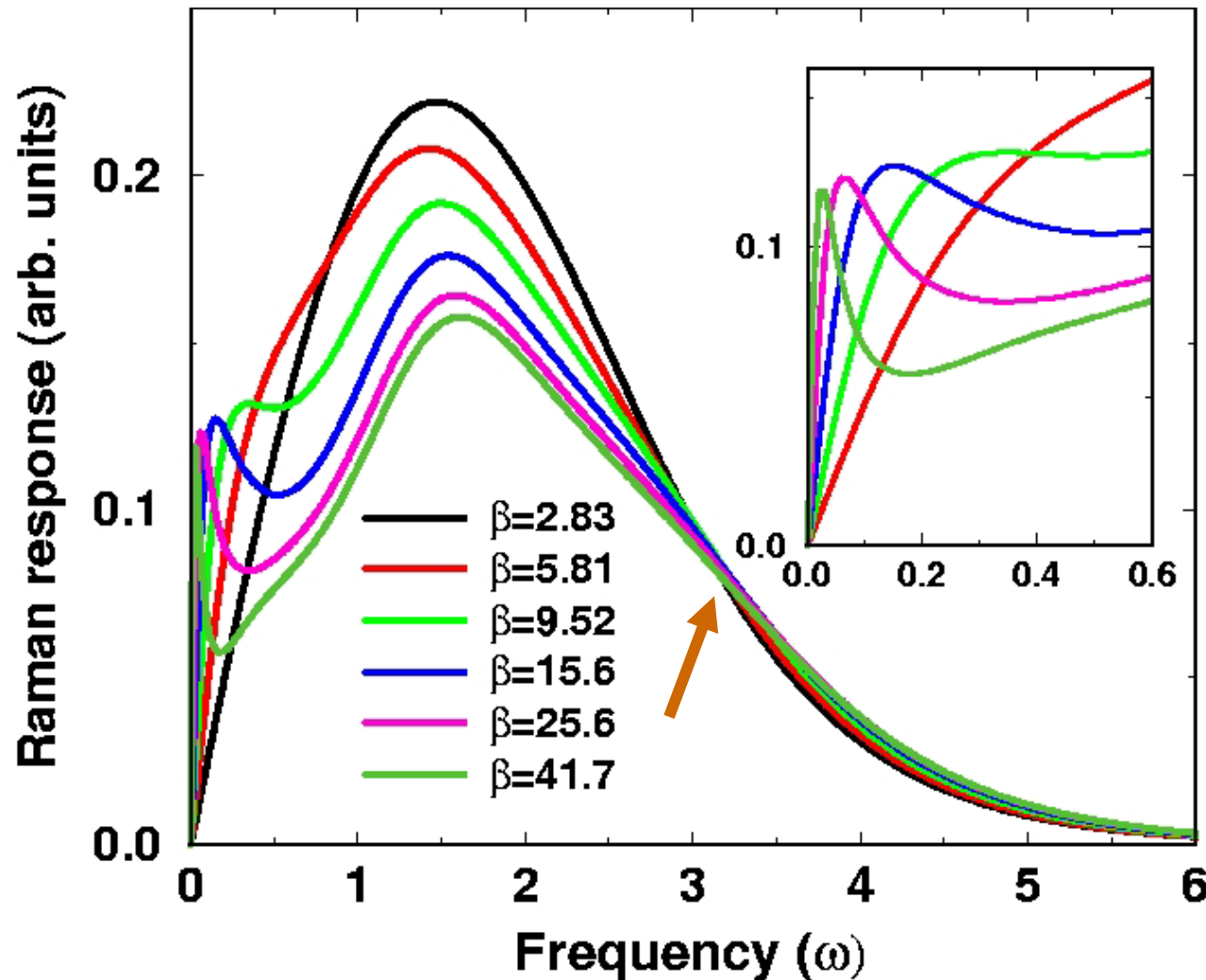
$$H = -\frac{t}{2\sqrt{d}} \sum c_{i\sigma}^* c_{j\sigma} + U \sum n_{i\uparrow} n_{i\downarrow}$$



Both electrons are now **mobile**

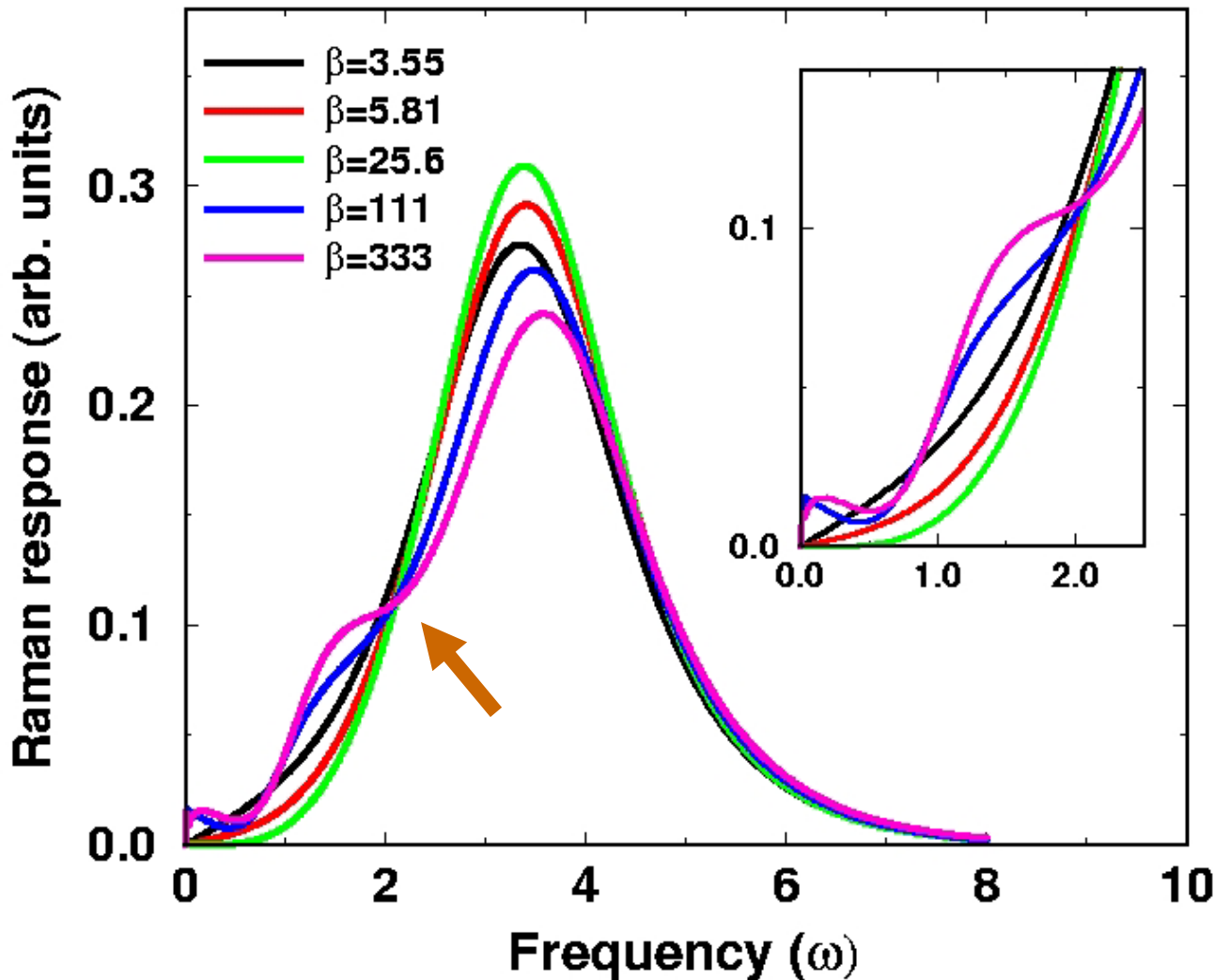
- **Exactly solvable** model on a hypercubic lattice in infinite dimensions using dynamical mean field theory (but requires **NRG** calculations to extract real frequency information).
- The irreducible charge vertex is **problematic to calculate** because it possesses too large a dynamic range for max-ent techniques.
- *Hence, the inelastic light scattering response can be constructed formally exactly for the nonresonant  $B_{1g}$  channel only (zone diagonal).*

# Nonresonant $B_{1g}$ Raman scattering ( $n=1, U=2.1$ )



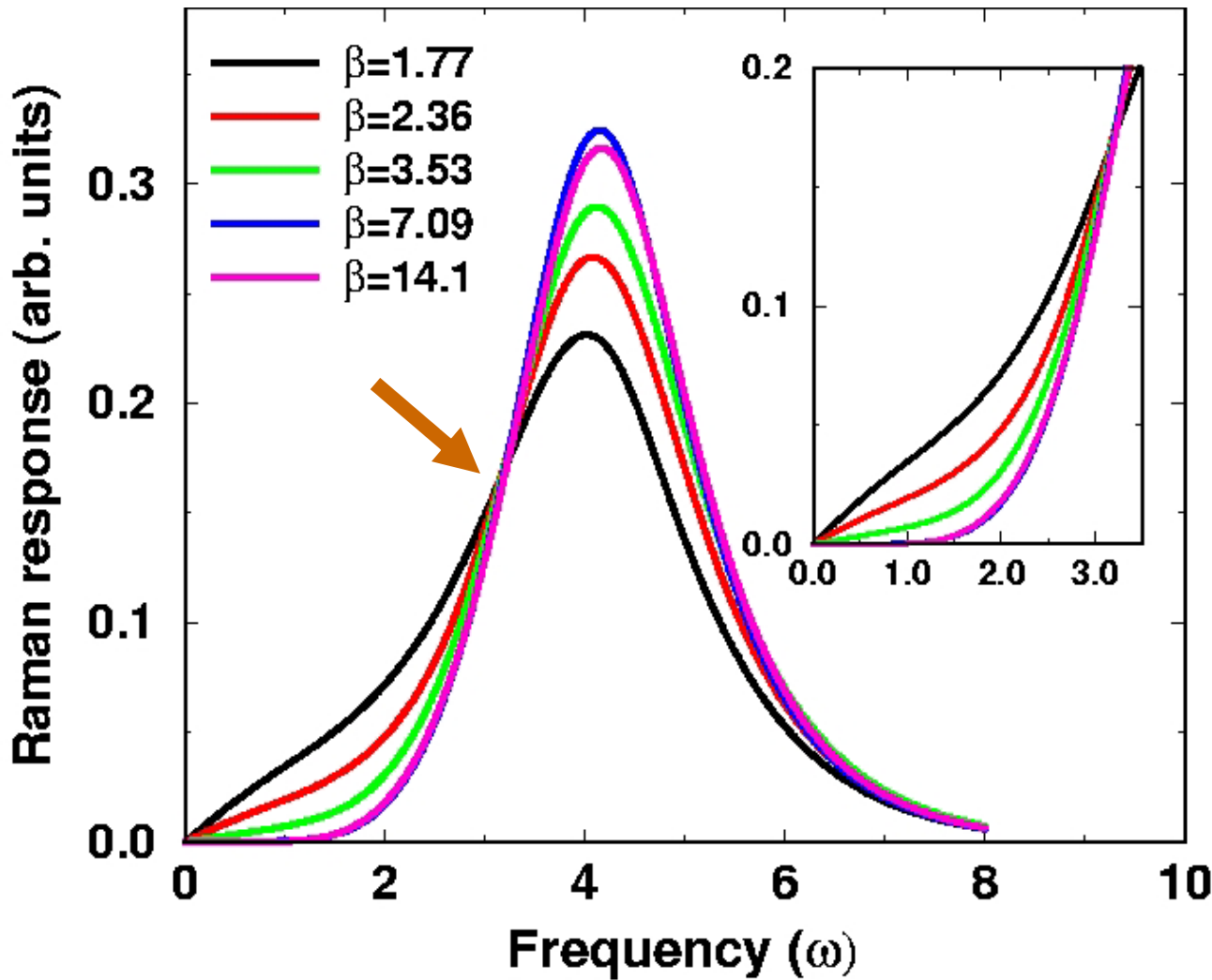
- Note the **charge transfer peak** as well as the **Fermi liquid peak** at low energy. As  $T$  goes to zero, the Fermi peak **sharpens** and **moves to lower energy**, as expected.
- There is **no low energy and low- $T$  isosbestic point**, rather a high frequency isosbestic point seems to develop.

# Nonresonant $B_{1g}$ Raman scattering ( $n=1, U=3.5$ )



- This is **quite anomalous!** A MIT occurs as a function of  $T$ . Note the appearance of the low- $T$  isosbestic point.
- The low energy Raman response has rich behavior, with a number of low energy peaks developing at low- $T$ , but **the low energy weight increases as  $T$  decreases here.**

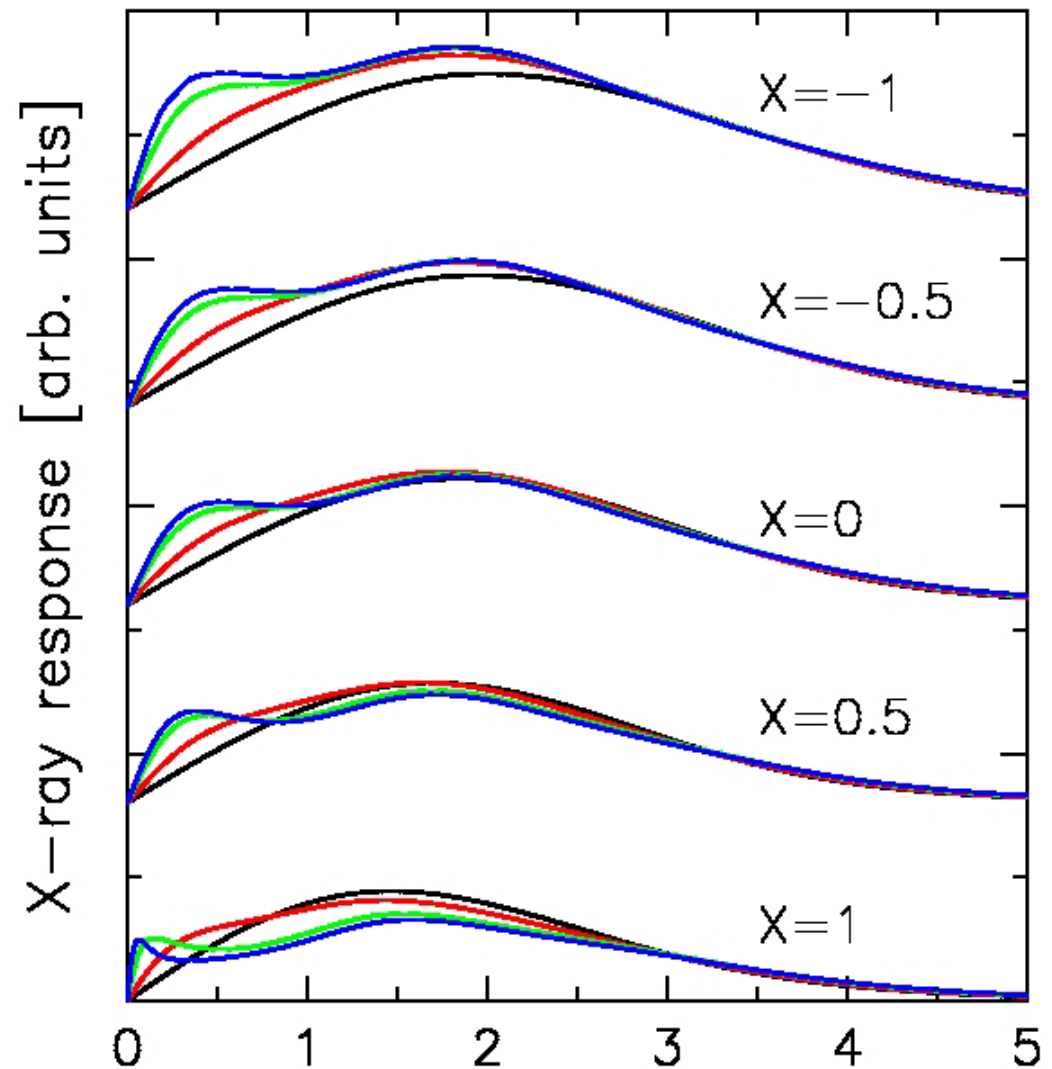
# Nonresonant $B_{1g}$ Raman scattering ( $n=1, U=4.2$ )



- Here we see the expected **universal behavior** for the insulator---the low-energy spectral weight is **depleted** as  $T$  goes to zero and an **isosbestic point** appears.
- The temperature dependence here is over a **wider range** than for the FK model due to the **T-dependence** of the interacting DOS.

# Inelastic X-ray scattering ( $B_{1g}$ , zone diagonal)

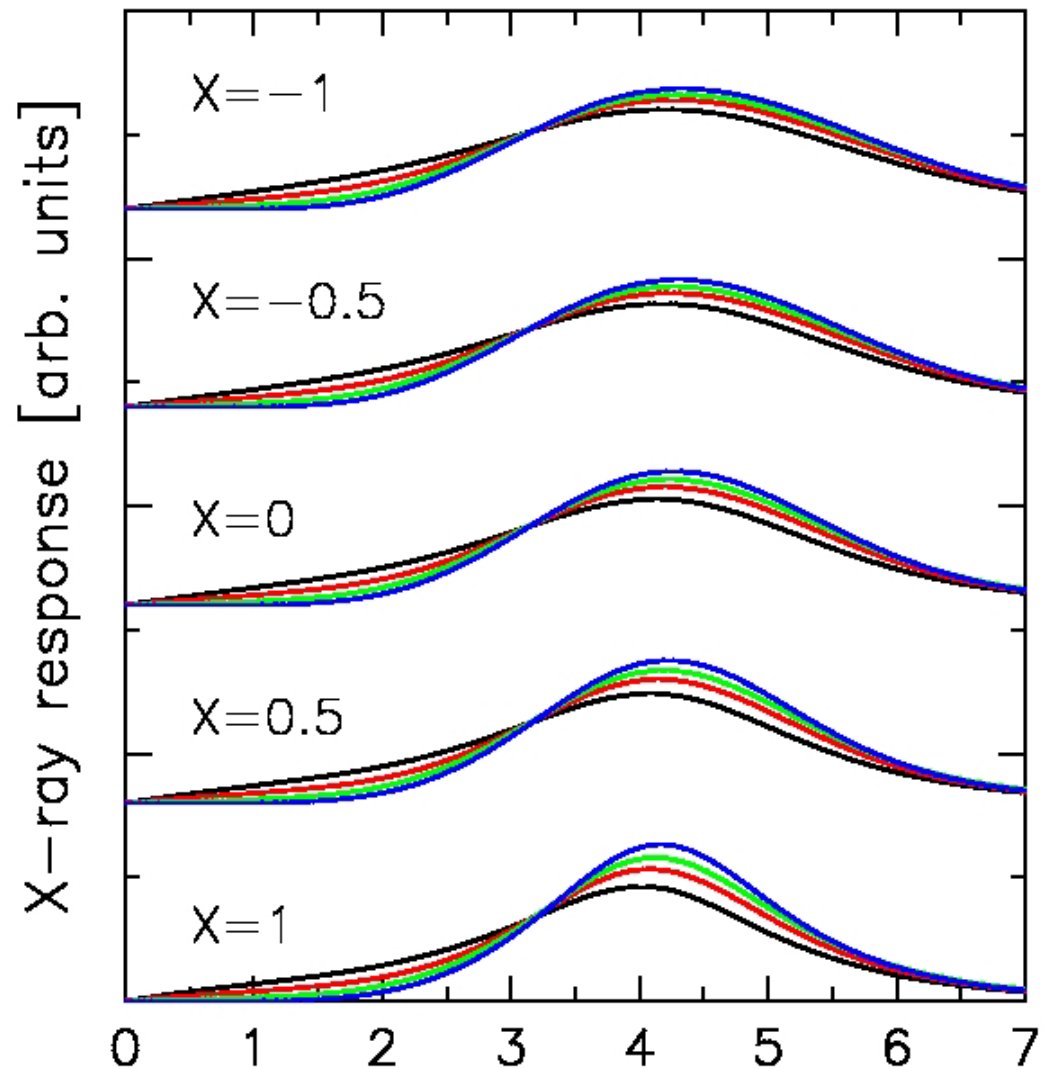
- Nonresonant scattering for a **correlated metal**, at half filling and  $U=2.12$ .
- Note how the Fermi peak **broadens** and **remains away from  $\omega=0$**  as  $q$  increases.
- The response functions at finite momentum transfer are all quite **similar**.
- There is a **small dispersion** of the peak locations.





# Inelastic X-ray scattering ( $B_{1g}$ , zone diagonal)

- Nonresonant scattering for a **correlated insulator**, at half filling and  $U=4.24$ .
- There is **no fermi peak** here because it is an insulator.
- Note how the main effect of finite-q scattering is to **broaden the charge transfer peak and shift it to slightly higher energy**.
- The isosbestic point **does not disperse** through the Brillouin zone.

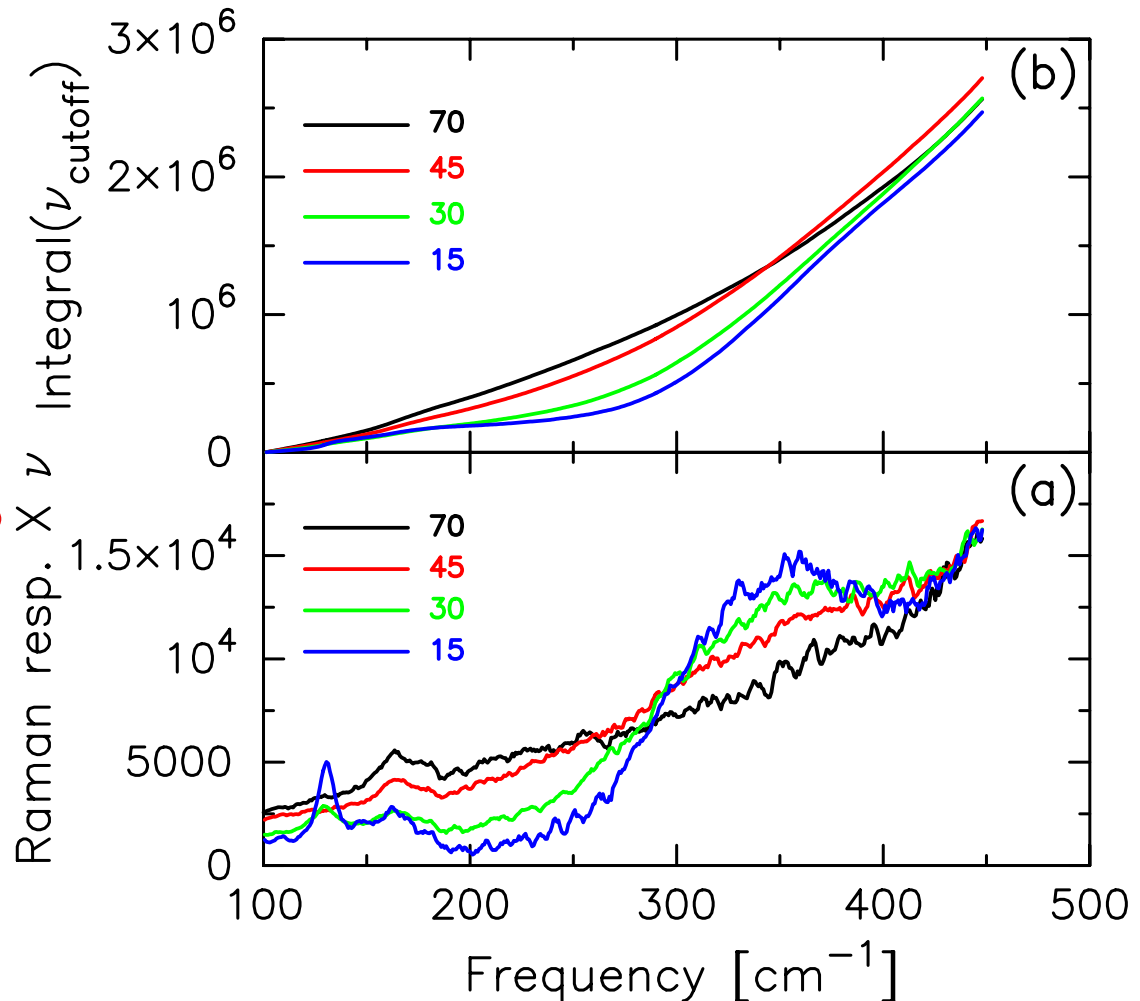


# Summary Hubbard model

- The Fermi-liquid behavior introduces new features to the  $B_{1g}$  Raman response: there is a characteristic **Drude like feature** that develops at the lowest frequencies (with a width that decreases like  $T^2$ ). This **low-energy spectral weight increases** as  $T$  decreases.
- In the insulating phase we see the expected “**universal behavior**,” in the Raman scattering but the temperature dependence is smoother here, because the interacting DOS is also  $T$ -dependent.
- When we transfer both momentum and energy from the photon, we find that the peaks are **generically broadened**, and there is **no evolution** of the fermi-peak.

# Sum rules for Raman scattering

- Data on  $\text{SmB}_6$  shows that the integral of the first moment of the Raman response satisfies a sum rule. It is almost a constant as a function of  $T$ .

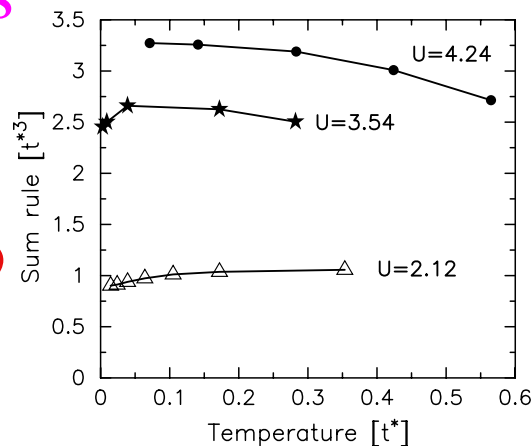
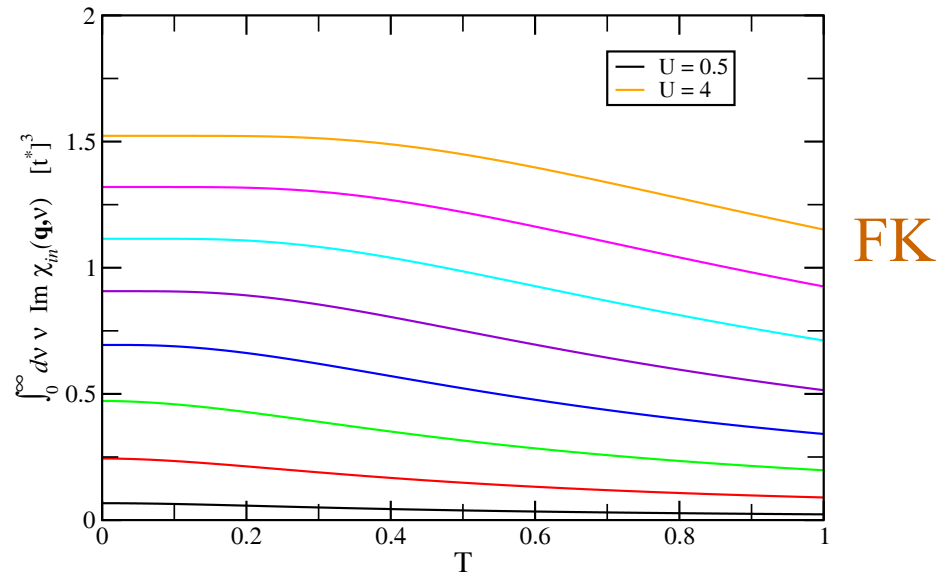


# Theory for the sum rule

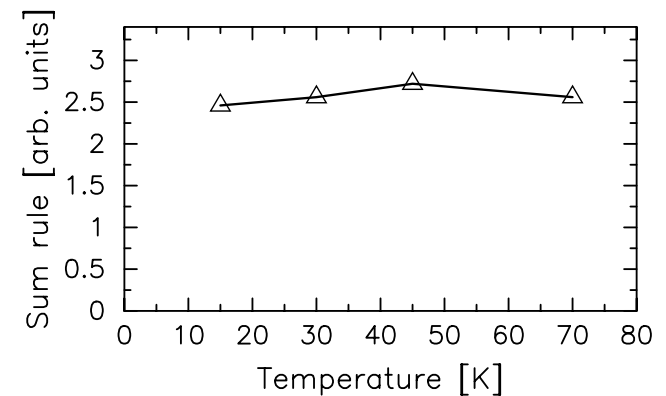
- A simple analysis of the nonresonant response function shows the **first moment** of the Raman signal is proportional to  $\langle [\rho_{\text{Raman}}, [H, \rho_{\text{Raman}}]] \rangle$ , with  $\rho_{\text{Raman}} = \sum_{\mathbf{k}} \gamma(\mathbf{k}) c_{\mathbf{k}}^{\dagger} c_{\mathbf{k}}$  the Raman density operator (stress tensor).
- Since the kinetic energy **commutes** with the stress tensor, the sum rule depends only on the **potential energy!**

# Results for $\chi''(\mathbf{q}, \nu)$

- The sum rule for the FK model is **almost constant** as a function of  $T$  at low  $T$ .
- For the Hubbard model, it appears to have a **low- $T$  decline**.
- This is similar to  $\text{SmB}_6$ .



Hubbard



$\text{SmB}_6$

# Conclusions

- Showed how an exact solution for **Raman** scattering can be constructed for a system that passes through a metal-insulator transition. The solutions displayed both an **isosbestic point** and a **rapid increase in low-frequency spectral weight** near the quantum-critical point, just as seen in experimental Raman scattering. There were interesting **resonant effects** too.
- Results are **model independent** or “**universal**” on the insulating side of the metal-insulator transition, explaining why so many different correlated insulators show similar behavior.
- Found a new **sum rule** for inelastic light scattering that provides information about the **potential energy** of the material.